An online surface defects detection system for AWAM based on deep learning

Shangyong Tang*, Guilan Wang*, Haiou Zhang**, Rui Wang**

* State Key Laboratory of Materials Processing and Die & Mould Technology, Huazhong University of Science and Technology, Wuhan 430074, PR China
** State Key Laboratory of Digital Manufacturing Equipment and Technology, Huazhong University of Science and Technology, Wuhan 430074, PR China

Abstract

Defects detecting layer by layer in arc welding based additive manufacturing (AWAM) is a big challenge as it affects the successive layer quality of the products. Most of the work on layer quality defection were focused on 3D profile measurement and X-ray spectroscopy method but it is inefficient, expensive with poor adaptability. In this work, an online intelligent surface defects detection system for AWAM was developed through deep learning algorithm and support vector machine method. To achieve a reliable surface feature of the welding beads, a vision sensor was used to get the image of the shaped surface synchronously. The system was trained offline and online to acquire knowledge of the welding beads which were classified into five patterns as normal, pore, hump, depression and undercut. An defection test result showed 95.29% accuracy. The system was verified to be practical with high accuracy and efficiency for the surface defects.

Introduction

Metal additive manufacturing (AM) has got great interest in recent years due to its numerous advantages against traditional manufacturing [1]. The process in arc welding based additive manufacturing (AWAM) is outstanding as its high deposition rate, cost competitiveness, and environmental friendly especially in fabricating large component [2]. But there are so many factors that affect the forming quality such as splash, arc disable, smoke, heat and electromagnetic interference. The defects appeared are damaged for the next layer and for the whole product. The quality of current layer is the foundation next layer's quality and stability. It will have an irreversible effect on the overall quality of the forming part once a surface defects are not detected and processed in a layer.According to a roadmap on the measurement science for metal AM [3],[4] hosted by the National Institute of Standards and Technology (NIST), closed-loop control systems for AM was identified as an important technology and measurement challenge. Part quality in AM is highly variable thereby limiting AM's broad acceptance. It is quite necessary to establish a monitoring system for the AWAM to avoid defects as it affects the successive layer quality of the product.

Most of the work on layer quality defection were focused on 3D profile measurement, X-ray spectroscopy method, magnetic leakage method, ultrasonic wave and infrared thermal image. The group at the Katholic University of Leuven measured both melt-pool geometry and infrared (IR)

radiation intensity signal [5],[6] and found that the melting process is influenced by more than 50 parameters, which are a significant challenge for monitoring or controlling all parameters. Dinwiddie et al. developed a high speed IR thermographic system to detect porosity for a electron beam machine [7]. However, the images could not be converted to true temperatures as there was no temperature calibration. Santosprito et al. describe a thermography based system to record the movement of heat movement [8] as defects (cracks, porosity, etc.) create lower conductivity regions and affect heat flow. However, since the changes due to these defects are small, it's quite limited by the type of defect and the adaptation of the analysis algorithm. Abd-Elghany and Bourell equipped with an energy dispersive X-ray (EDX) analyzer to evaluated the surface finish of the PBF processed part [9]. They found that the large amounts of particles had a tendency to form voids when they were removed in post-processes. Ding Y et al. developed a laser-based machine vision measurement system to measure the 3D profile of deformed surface [10],[11]. The deformed plate was calculated for bending analysis and transverse shrinkage based on the 3D profile data.But the surface defects were difficult to analyze as there were too much interference signal and the details of the surface were difficult to handle. All the methods above were used to detect the physical properties of the defections to evaluate the status of the product. Only a number of special types of defects could be detected by a single method along with limitation of application environment and the analysis algorithm was quite complicated. Some methods needs special using environment on the surface and cost highly with complexity.A new efficient, adaptable and cheap detective method for surface defection on additive manufacturing is quite necessary.

With the continuous progress of machine vision technology, machine vision is being paid attention widely as a new method for surface detection. Liu, RW investigate a stereo vision-based hybrid manufacturing process to repair metallic components automatically [12]. It can repair metallic components with large defect area range but no defect details. Aminzadeh et al. established a system to capture 2D optical images from each layer of the AM part during the build to analyze and detecte the geometric errors, surface defects and the dimensional accuracy in each layer [13]. The method based on machine vision has the following advantages.

(1) The machine vision inspection is non-contact measurement with strong applicabilit.

(2) The images collected contain abundant of surface information.

(3) The adaptability of the algorithm can make the whole system more adaptable.

The connection of the detection system is shown in Fig. 1. A industrial computer was used to control the robot and set the welding Parameters of the welding power machine. The melting surface information was acquired with a specific light source and sensor assistance through the machine vision. The image signal is processed and analyzed by the computer in real time. An image processing algorithm was used to process the surface image information to obtain the required defect characteristics. The selected features was used to reason, predict or identify the surface defects.

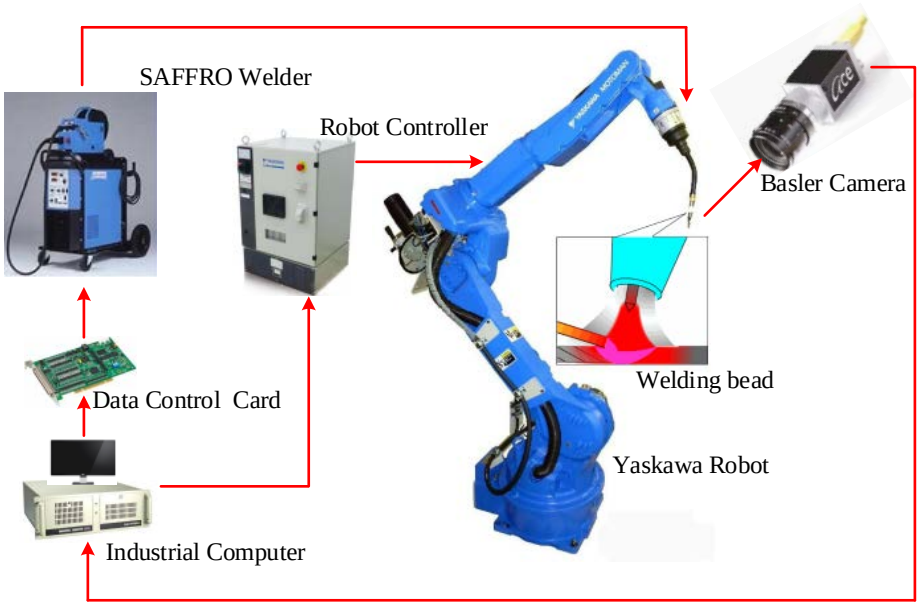

Fig.1 Diagram connection of the detection system.

A single algorithm with machine vision is not adaptable. An algorithm with better adaptability is need for the image processing of surface defection. Aviles-Viñas J F et al. proposed an architecture based on an artificial neural network (ANN) to learn welding skills automatically in industrial robots [14]. The image information of welding beads can be handled with an adaptable but not complex algorithm. This is due to the strong adaptability of the neural network structure. Vahabli E et al.[15] proposed a new methodology based on radial basis function neural networks (RBFNNs) to improve the surface roughness of parts fabricated. In order to get a good adaptive algorithm for identification of surface defects, the deep learning based on neural network is combined with image processing to solve the problem of poor adaptive algorithm. The whole algorithm structure does not need to change to increase a new defect mode.

The mode we designed for surface detection is shown in Fig. 2. The camera is behind the touch for tracking and scanning the shaped parts and acquiring the entire surface information of the weld bead. The image is processed using the deep learning algorithm to analyze the type of welding beads and quality of beads information.

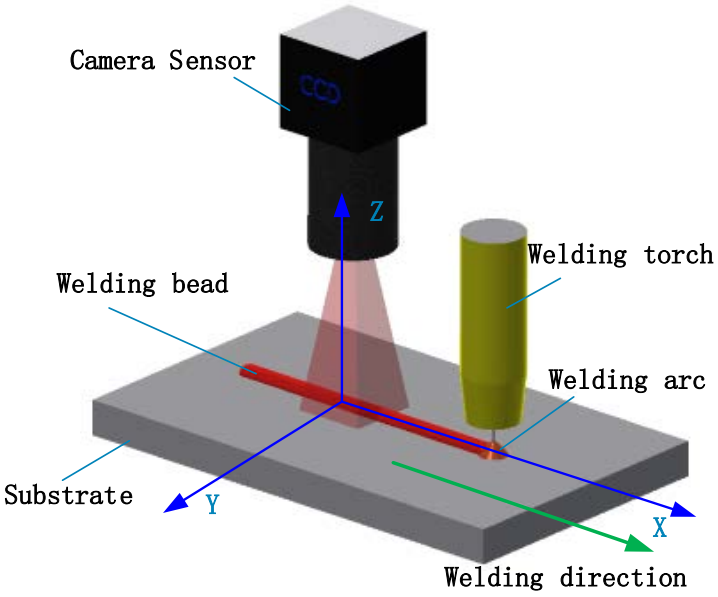

Fig.2 The structure of camera acquisition and detection system

In this paper, the welding direction is set as x direction, accumulation direction as z direction and the horizontal direction perpendicular to the x direction as y direction. The camere sensor moved along the x direction (scanning direction) so that the sensor can get the full information of the deformed surface. Then a surface image data of the measured surface was collected and analyzed.

Research methodology

1 Convolutional Neural Networks and Support Vector Machine

Convolutional neural networks (CNN) is a deep learning method developed in recent years in the field of speech analysis, image recognition and other fields. It uses a convolutional layer and a subsampling layer in a paired manner so that it has a high degree of invariance for translation, scaling, tilting, or other forms of deformation. At the same time, it creatively uses the receptive field and weight sharing to reduce the number of parameters needed to train in the network. It also makes it different from other machine learning methods as it simplify the network structure and the two-dimensional image can be directly used as input which greatly simplifies the preprocessing process.

CNN is a multi-layer neural network, as shown in Fig. 3. Each layer consists of multiple two-dimensional planes, consisting of multiple independent neurons. In general, the convolution layer (C) responsible for feature extraction is always paired with the subsampling layer (S) responsible for local averaging and secondary extraction. This approach increases the number of layers of the network while increasing the tolerance to the input samples. When the number of network layers

is too large, the gradient of the error will be diverged in layers and the residual from the post-transmission to the front will get smaller during the backpropagation (BP) stage of training. This will result in faster convergence near the output layer of the network layer and slower convergence away from the output layer of the network layer.

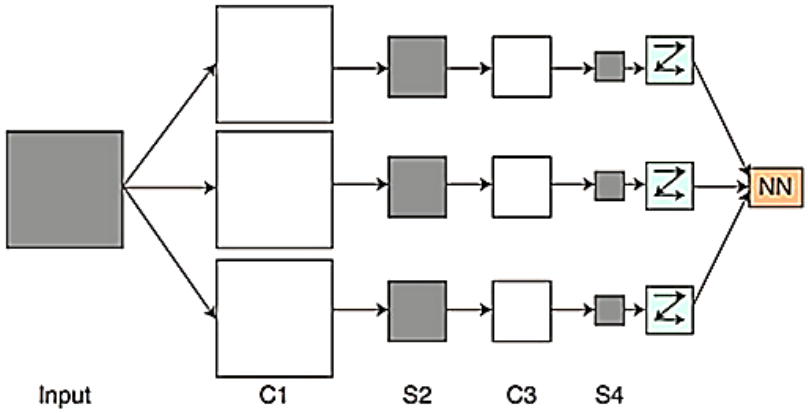

Fig.3 The structure of convolutional neural networks(C1 and C3 represent convolution layers, and S2 and S4 represent subsampling layers.)

CNN's convolution and subsampling layers can be regarded as feature extraction layers. The output layer consists of a European radial basis element and can be used directly as a classifier. Therefore, the CNN has a feature extraction function with a classification function for input directly. In order to obtain a better classification performance, the CNN of which the output layer is removed is used as the feature extractor, and the output vector of the fully connected layer of the penultimate layer is taken as the input of the feature vector of defect image in this article. This kind of feature vector samples are trained for Support Vector Machine(SVM) for better classify ability. The flow of the feature extractor is shown in Fig. 4.

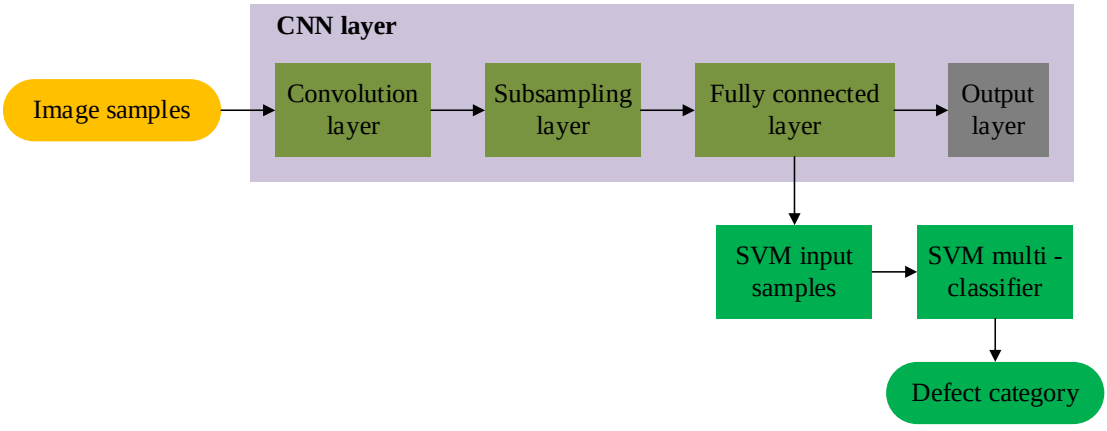

Fig 4. The flow chart of feature extractor of CNN

SVM is developed as a linear classifier, but the classification of image processing is non-linear

and in high-dimensional space. It can achieve excellent characteristics on nonlinear problems by linear mapping. In dealing with nonlinear classification problems, SVM maps a sample to a high-dimensional linear space by applying a fixed nonlinear mapping, so that the nonlinear problem can be solved by the optimization method of linear problem. This kind of non-linear mapping is called a Kernel function. Gaussian kernel function is one of the most commonly used kernel functions in practical application. Its separability and locality make it easy to achieve satisfactory results when solving practical problems. The classification performance of SVM is closely related to the type of kernel function. The parameter selection and the size of the penalty coefficient C of kernel function are also an important factor that affects the performance of SVM. In this paper, we used a Gaussian kernel function to transform the eigenvector. The parameters that need to be optimized were Gaussian kernel radius σ and penalty coefficient C. The general form of the Gaussian kernel function is as follows.

$$K(x, x_i) = exp[-\| x - x_i \|^2 / (2\sigma^2)],\ \sigma > 0 \text{ is kernel radius.}$$

There are many ways of SVM classification, including one against rest, one against one and two-branch methods. In this paper, we used a two-branch method to be a classifier, which was also known as decision tree method. The basic idea of two-branch method is to divide the class contained in the top root node into two subclasses, and then divide the two subclasses until the subclass contains only one class, that is, all the categories in the original sample have been divided. The final shape is a binary tree and each node of the binary tree is a support vector machine classifier. The binary tree has the least number of classifiers and fast speed of decision making. But the main problem is that when the top classifier has a misjudgment, the classification result which is wrong has nothing to do with subsequent judgment, and the error rate of each classifier has related to the division of the subclass, that is to say, the construction of a binary tree is an empirical work and need a lot of tests.

In this work, 2040 samples were used for the training of SVM classification. There were 783 normal samples, 438 samples for pore defects, 324 for hump defects, 297 for depression and 198 for undercut defects. In these five types of samples, the undercut defect is relatively scarce because of the less appearance in the actual arc welding process. The other four types of samples have a more balanced distribution. In the construction of binary tree, the following principles should be considered based on the past experience.

(1) The classes that were distinguishable easily should be separated earlier to ensure better generalization ability of the top-level classifier.

(2) The classes that were wide range should be separated earlier so that it could occupie a larger area of the division.

(3) The classes that were important and rare should be separated earlier so that the classifier could have a higher search rate for these two important categories.

Considering the difference of sample number distribution, the difference of sample image characteristics and the difference of category importance, we designed a structure of binary tree of

SVM method to classify the arc deposition surface defects, as shown in Fig. 5. The structure was a classifier that allowed two subclasses which were both multi-class combinations. What considered mostly was the balance of the sample size and the difference between subclass image features in each classifier combination. The normal sample and the depression defect sample make up the first subclass. The pore defect samples, hump defect samples and undercut defect samples make up the second subclass. The sample size of two subclasses was equivalent. The normal sample is more closely to the hump defect samples in the visual image of the sample. The pore defect and the undercut defect were both defects of holes except the difference between size and quantity. The similar categories were placed in two subclasses to improve the sample differences in subclass classification.

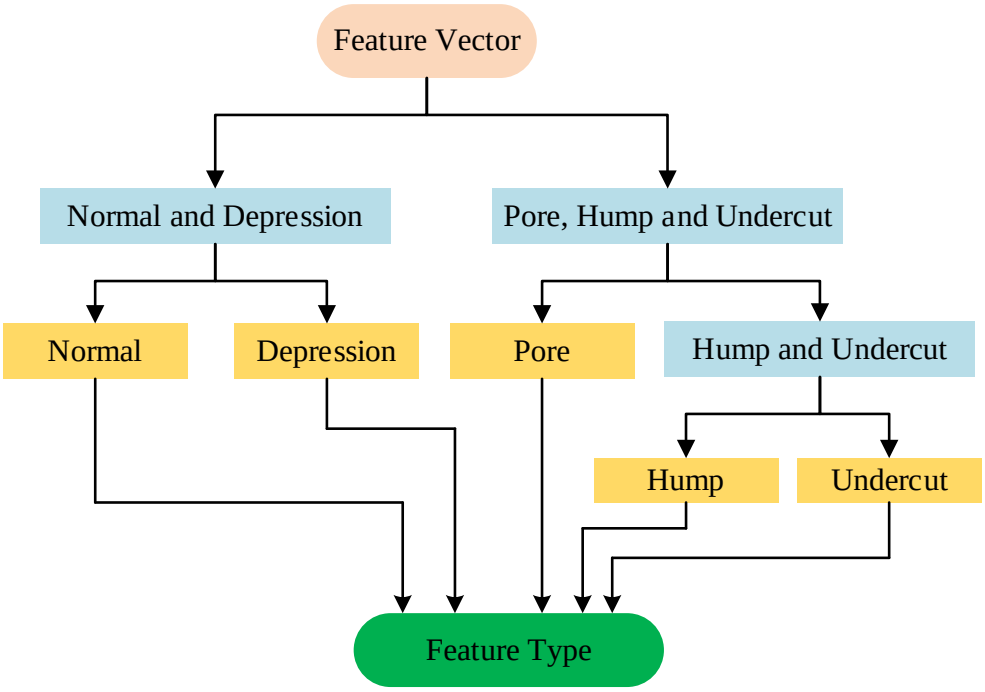

Fig. 5. Structure of binary tree of SVM method

2 The training process of CNN

The essence of convolutional neural networks is the mapping of input vectors to output vectors. It learns this mapping relationship from a large number of input samples instead of providing precise mathematical expressions between input and output. It takes a form of supervised learning, and its training and test samples are vector pairs which are made up of the input vector and the ideal output vector. All the samples were collected from the reality experiment. The output error was calculated by comparing the actual output vector of the input with the ideal output vector. Then the training of CNN was followed by a traditional BP algorithm, which was divided into two stages as follows.

The first stage was the forward propagation phase.

(1) Take a sample X (X_p,Y_p) and input X into the network.

(2) Calculate the actual output Q_p of X sample.

The second stage was the backward propagation (BP) phase.

(1) Calculate the deviation of the actual output Q_p from the ideal output Y_p.

(2) Update weight matrix by back propagation through the minimization error method.

In the first stage, the forward propagation phase is the same as the general neural network. Each layer of neurons on CNN calculates the weight of the upper layer of neurons connected to it. The output of current neuron is calculated by the activation function shown in the follows.

$$h_{W,b}(x) = f(u), \quad \mathrm{u} = \mathrm{W}^{\mathrm{T}}\mathrm{X} = \sum_{i=1}^{i=n} W_i x_i + b \tag{1}$$

The $h_{W,b}$ represents the output of neuron, and f(u) represents the threshold function, which was 1.7159tanh（2x/3）in our CNN model. W_i represents the weight of the i-th connection, b represents the offset of the current neuron, x_i represents the output value of the neuron connected.

The actual output can be obtained by calculating the output of each neuron from the CNN layer by layer. The square error is used as the cost function, the sample class has a total of c, and the sample size is N. The cost function is shown below.

$$E^N = \frac{1}{2}\sum_{n=1}^{N}\sum_{k=1}^{c}\left(t_k^n - y_k^n\right)^2 \tag{2}$$

The E^N represents the squared error of the sample, t_k^n represents the k-dimension of the corresponding label for the n-th sample,y_k^n represents the k- dimension output of the n-th sample in CNN. The squared error of the samples is the sum of the squared error of a single sample, and the backward propagation process of only a individual sample need to be considered. The squared error of the n-th sample is expressed as follows.

$$E^n = \frac{1}{2}\sum_{k=1}^{c}\left(t_k^n - y_k^n\right)^2 \tag{3}$$

In the forward propagation phase, the deviation between the actual output and the theoretical output can be obtained by calculating the output of each neuron. The neural network can adjust the weight to reduce the deviation between the actual output and the theoretical output through the backward propagation of the deviation. The deviation of backward propagation can be seen as the sensitivity of the base of each neuron, which is defined as follows.

$$\frac{\partial E}{\partial b} = \frac{\partial E}{\partial u}\frac{\partial u}{\partial b} = \delta \tag{4}$$

It can be seen from equation (1) that $\partial \mathrm{u}/\partial \mathrm{b} = 1$, so $\delta = \partial \mathrm{E}/\partial \mathrm{u}$. That is, the sensitivity of the base δ and the derivative of the error E for a input u of a node is equal. This derivative is the key to getting the top-level deviation propagate back to the bottom. The sensitivity of each layer can be

expressed as follows.

$$\delta^l = \left(W^{l+1}\right)^T \delta^{l+1} \square f'\left(u^l\right) \tag{5}$$

δ^l represents the sensitivity of l-th layer, W^{l+1} represents the connection weights of (l+1)-th layer. The sensitivity of the output layer is expressed as follows.

$$\delta^L = f'\left(u^L\right) \square \left(y^n - t^n\right) \tag{6}$$

Finally, the weights is updated for each neuron by using the sensitivity. As shown below.

$$\frac{\partial E}{\partial W^l} = x^{l-1}\left(\delta^l\right)^T, \quad \Delta W^l = -\eta \frac{\partial E}{\partial W^l} \tag{7}$$

x^{l-1} represents the output of upper layer.

3 The structure of CNN

The structure of CNN is shown in Fig. 6 with a total number of 7 layers including the input layer and output layer. There are 4 feature extraction layers from layer 1 to layer 4, and layer 5 is the fully connected layer. The image size of input layer is 85×107. Layer 1 uses a 5×5 convolution to do feature extraction for input layer with a horizontal and vertical moving distance of 2 steps and get 3 feature maps of 41×53. Layer 2 uses a 5×5 convolution to do feature extraction for Layer 1 with a horizontal and vertical moving distance of 2 steps and get 6 feature maps of 19×25. Layer 3 uses a 5×5 convolution to do feature extraction for Layer 2 with a horizontal and vertical moving distance of 2 steps and get 12 feature maps of 8×11. Layer 4 uses a 3×4 convolution to do feature extraction for Layer 3 with a horizontal moving distance of 2 steps and vertical moving distance of 1 steps and get 18 feature maps of 5×5. Layer 5 is connected to Layer 4 with a full connection, and the output layer is also connected to Layer 5 through a full connection.

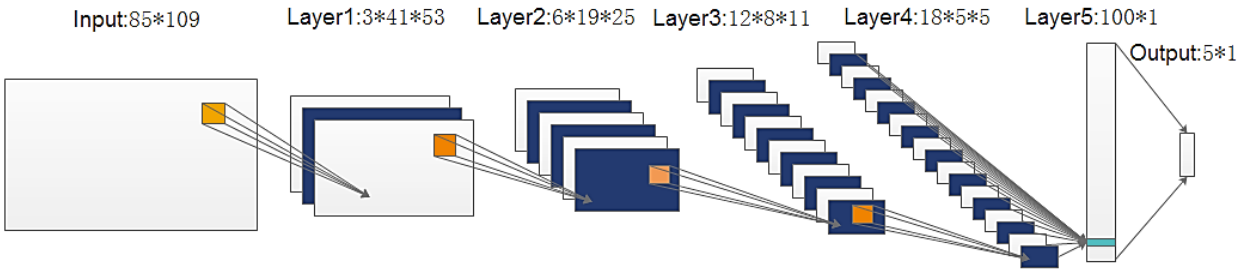

Fig. 6 Structure of CNN

In the connection between Layer1 and Layer 4, an incomplete connection mechanism is adopted to keep the number of connections within a reasonable range and destroy the symmetry of the network. This makes the input of different feature maps to be different and forces them to extract different characteristics from the previous layer. The connection of network map between

Layer 1 and Layer 2 is shown in table 1. The connection of network map between Layer 2 and Layer 3 is shown in table 2. The connection of network map between Layer 3 and Layer 4 is shown in table 3.

Table 1.Connection of network map between Layer 1 and Layer 2

		Layer 2					
		1	2	3	4	5	6
Layer1	1	●	●		●	●	
	2	●		●	●		
	3		●	●	●		●

Table 2.Connection of network map between Layer 2 and Layer 3

		Layer 3											
		1	2	3	4	5	6	7	8	9	10	11	12
Layer 2	1	●				●	●	●			●	●	●
	2	●	●				●	●	●			●	●
	3	●	●	●				●	●	●			●
	4		●	●	●			●	●	●	●		●
	5			●	●	●			●	●	●	●	●
	6				●	●	●			●	●	●	●

Table 3.Connection of network map between Layer 3 and Layer 4

Layer 3 \ Layer 4	1	2	3	4	5	6	7	8	9	10	11	12
1	●	●	●	●	●	●						
2		●	●	●	●	●	●					
3			●	●	●	●	●	●				
4				●	●	●	●	●	●			
5					●	●	●	●	●	●		
6						●	●	●	●	●	●	
7							●	●	●	●	●	●
8	●	●	●				●	●	●	●		
9		●	●	●				●	●	●	●	
10			●	●	●				●	●	●	●
11	●			●	●	●				●	●	●
12	●	●			●	●	●				●	●
13	●	●	●			●	●	●				●
14	●	●	●	●			●	●	●			
15	●	●	●	●	●	●				●	●	●
16	●	●	●	●	●	●	●				●	●
17	●	●	●	●	●	●	●	●				●
18	●	●	●	●	●	●	●	●	●	●	●	●

Results and discussion

The original image is collected by using a CMOS sensors. Part of the sample image is shown in Fig. 7. In order to obtain the realistic image information, the input image was preprocessed to

improve the image's signal-to-noise ratio (SNR). The preprocessing flow of the input image is shown in Fig 8.

Fig. 7 The defected image of selected ROI. The type of defection from top to bottom is normal, pore, hump, depression and undercut

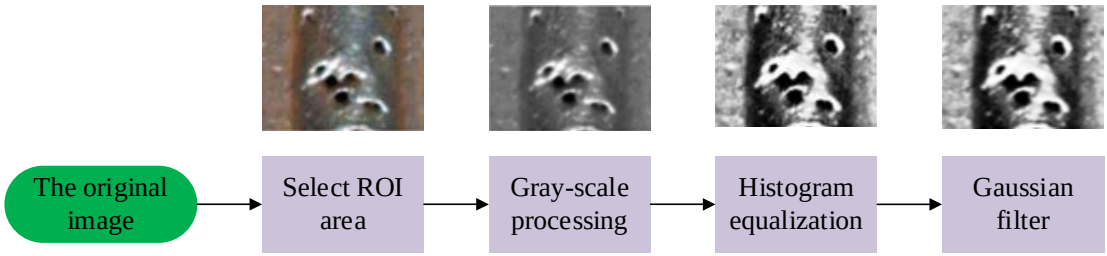

Fig. 8 The flow of image preprocessing

The original image is a three-channel color image. The input image was converted into a single-channel grayscale image for ease processing. The gray distribution of images obtained from the same surface through industrial cameras in different lighting conditions or shooting angles can also be different. The grayscale image was under histogram equalization in order to minimize the grayscale change caused by the external environment and enhance the detail contrast of the image. The substance of histogram equalization is that, carrying out nonlinear extensionof the image and redistributing the image gray value to make it into a uniform distribution within the scope of all gray for the the area where the grayscale of the original image is relatively concentrated. This method can enhance the local contrast of the image while making the overall gray distribution of the image more balanced and different samples of the same location less different. The image was Gaussian filtered in the last step by using a 5×5 filtering window for discretizing convolution to eliminate the Gaussian noise and obtain the image with a higher SNR. The feature maps extracted

by CNN network is shown in Fig. 9.

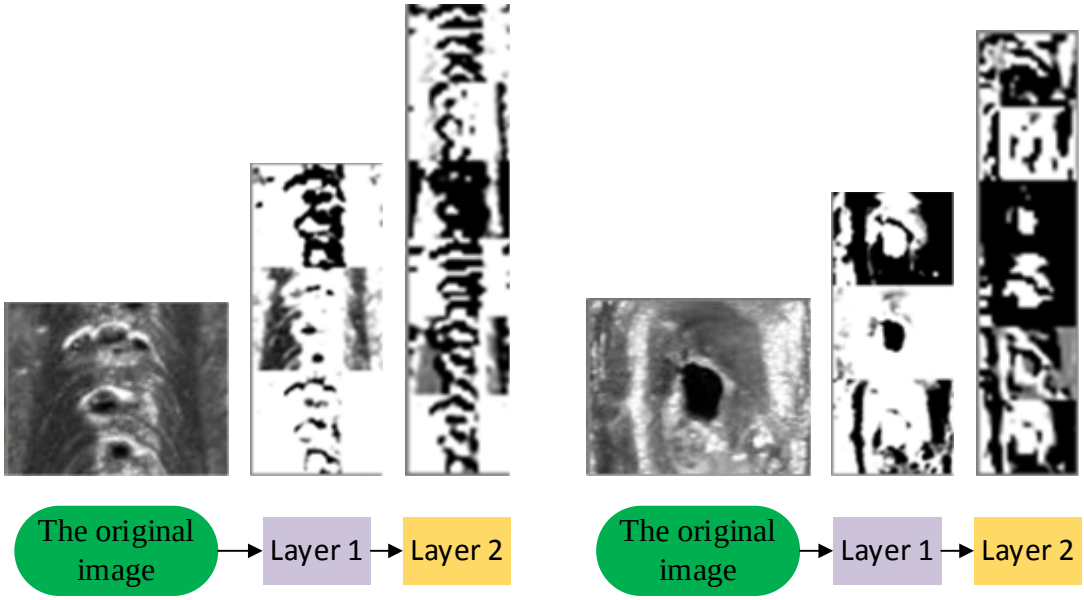

Fig.9 Two sets of feature maps

In the training samples, there were 1530 samples of normal, pore, hump, depression and undercut. These samples were far from enough for complex and variable arc welding surface defects. In the case of small sample size, the existing samples were deformed to increase the number of training samples and make the network more accurate in feature extraction of the samples. Before the training of the samples, three types of deformation were applied to the samples: proportion factor, rotation and elastic deformation. The original samples were enlarged or compressed in horizontal and vertical direction by applying different scaling factors in horizontal and vertical direction. The original samples were rotated clockwise or counterclockwise at a small angle to simulate more actual sample of acquisition status. The elastic deformation is based on the treatment of Dr. Simard. All the three deformations were linearly deformed. The transformation matrix could be generated and superimposed. A new training sample was obtained by multiplying the original sample matrix with the transformation matrix. The samples were deformed before training so that the samples trained in each iteration were not the same. Although this method of increasing the diversity of the sample reduces the convergence rate and increases the convergence error, the generalization ability of convolution neural network is improved. This makes it more accurate in dealing with real samples.

The deformed sample increases the sample diversity but reduces the convergence rate. We can make the network have a better convergence results by disrupt the distribution of its category labels for each iteration of the training sample, that is, randomized sample sequence. The network usually learns faster from unexpected samples. If the two samples are similar, the information that the small network can learn is limited because of the small error gradient. The adjacent samples are of different categories to increase their differences by randomizing the sequences. At the same time,

randomization also brings noise to the weight gradient update. This reduces the probability that the CNN falls into a local minimum, which means that the model is more likely to find deeper local minimums, that is, the smaller cost function value. The model can get better fit ability. The convergence of the sample sequence before and after randomization is shown in Fig. 10 and the test results of the sample sequence is shown in table 4. The big difference of the samples leads to the larger mean square error (MSE) of the initialized randomized training. But the network can get a good convergence result very quickly and the MSE was approache to 0.03 in the twentieth iteration. The MSE of the network training without randomization had been oscillating and the reduction is relatively slow.

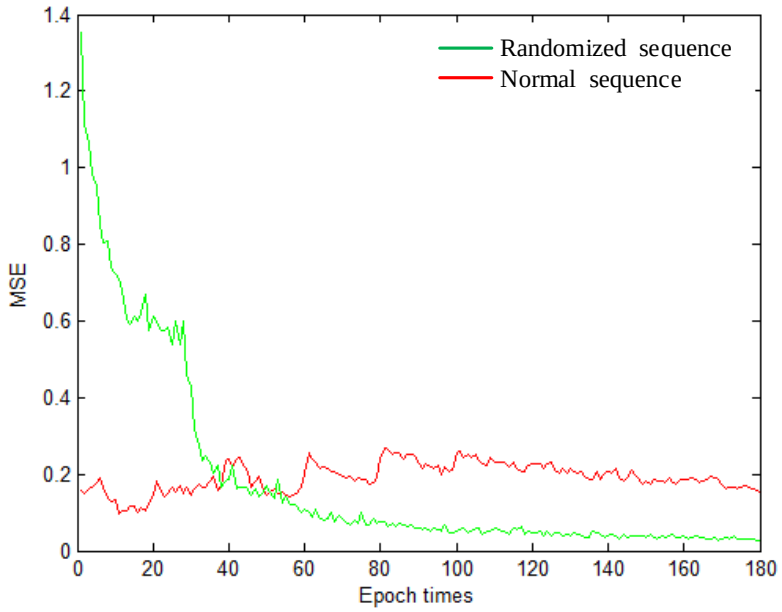

Fig. 10 The convergence of the sample sequence before and after randomization

Table 4 The test results of the sample sequence before and after randomization

	Accuracy of training	MSE of training	Accuracy of test	MSE of test
Normal	100%	0.0007771	86.84%	0.541116
Randomized	99.21%	0.0206215	94.45%	0.258445

A total of 1530 samples were randomly selected for convolution neural network training and the remaining 510 samples were for network testing. All the gray values of the sample data were homogenized to [-1,1] interval before training. The white was 1 and the black was -1. The mean of the input variables was close to zero to speed up the convergence rate. The Hessian matrix was updated and the learning rate was attenuated every 30 iterations during the training.

Six layers of network structure and seven layers of network structure were used for training to compare the neural network performance of different depths. The training results are shown in Fig 11 and table 5. The seven layers of network structure was slightly worse and the variance was

greater in the beginning of the training phase compared to six layers of network structure. This was because the seven layers had more neurons, connections and weights. The network structure advantage of the greater depth was reflected as the number of iterations increases. The mean variance of the six-layer network structure was stable at 0.02, and the mean variance of the seven-layer network structure was stable at 0.01. The test results of two network structures for the same test samples were shown in table 5. It can be seen that the generalization performance of the seven layer network structure is better for the test samples.

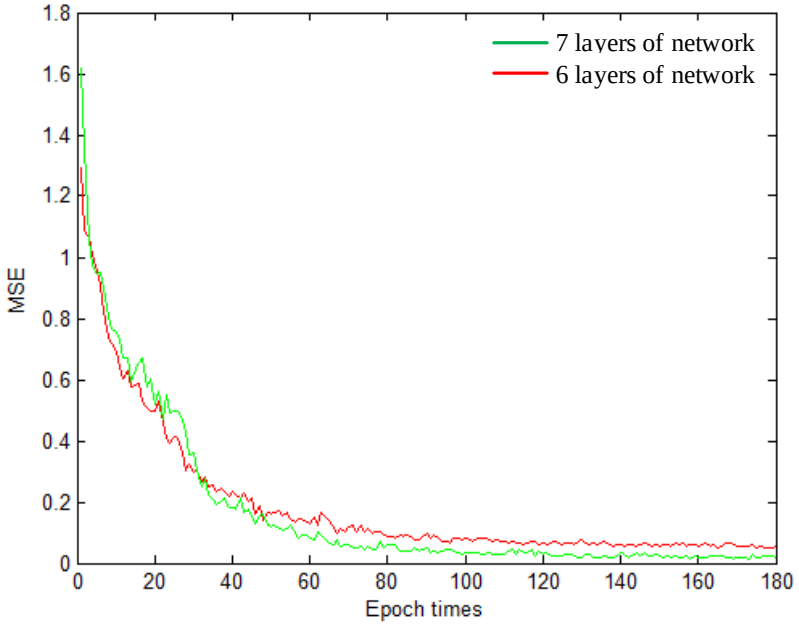

Fig 11 The convergence of different kinds of network structure

Table 5 The test results of different kinds of network structure

	Accuracy of training	MSE of training	Accuracy of test	MSE of test
Six layers	100%	0.0131734	92.35%	0.262467
Seven layers	100%	0.0105281	95.29%	0.260543

Conclusion

Aiming at the problem of defect detection of surface topography in arc welding based additive manufacturing, a detection and classification system that can be used for a variety of surface defects was developed. The system used an industrial CMOS camera to obtain a surface image of the layer surface. The input image was preprocessed to obtain the realistic image information and improve the image's signal-to-noise ratio. The support vector machine then classified the defects after the preprocessed image matrix was extracted by the convolution neural network. The surface defect of the image area was confirmed at last.

(1) The existing feature extraction and classification methods based on image has been

summarized. The surface defect detection system based on visual image and deep learning was designed and realized after the detailed understanding of the characteristics of different types of surface defects in arc welding based additive manufacturing.

(2) Considering that the image should contain as much information as possible without making the image size too large, the appropriate size of ROI area in the original image was extracted and preprocessed by using gray scale, histogram equalization, Gaussian filtering to improve the adaptability of the network in different environments.

(3) The method of extracting the feature directly from the input image based on the convolution neural network was proposed in case of contingent bad robustness by artificial extraction. The convolution neural network had a total of seven layers including three feature extraction processes and used the full connection layer neuron values as the eigenvector. The training results show that the method had a high degree of adaptability and the accuracy rate was 95.29%.

(4) A variety of strategies in the training process of CNN was used to improve the training accuracy and speed. A deformation method was used to increase the diversity and generalization ability of training samples and speed up the convergence rate and reduce the convergence of variance. The random sequence method and the second derivative method for changing the learning rate and feature map combination method was used in the training process.

(5) The SVM was used to classify the eigenvector after the extracting. The best SVM structure was determined using the LibSVM toolbox to optimize the parameters of SVM based on different conditions of the binary tree structure. An online defection test result showed that the system was verified to be practical with high accuracy and efficiency for the surface defects.

Reference

[1] Hofmann D C, Roberts S, Otis R, et al. Developing Gradient Metal Alloys through Radial Deposition Additive Manufacturing[J]. Sci Rep, 2014, 4(4):5357.

[2] Karunakaran K P, Suryakumar S, Pushpa V, et al. Low cost integration of additive and subtractive processes for hybrid layered manufacturing[J]. Robotics and Computer-Integrated Manufacturing, 2010, 26(5):490-499.

[3] Energetics Inc. for National Institute of Standards and Technology, Measurement science roadmap for metal-based additive manufacturing, May-2013.

[4] D. L. Bourell, M. C. Leu, and D. W. Rosen, Roadmap for additive manufacturing: identifying the future of freeform processing, Univ. Tex. Austin, 2009.

[5] Craeghs T, Clijsters S, Yasa E, et al. Online quality control of selective laser melting[J]. Proceedings of the 20th Solid Freeform Fabrication (SFF) symposium, Austin (Texas), 8-10 august, 2011.

[6] Craeghs T, Clijsters S, Kruth J P, et al. Detection of Process Failures in Layerwise Laser Melting with Optical Process Monitoring[J]. Physics Procedia, 2012, 39(39):753-759.
[7] Dinwiddie R B, Dehoff R R, Lloyd P D, et al. Thermographic in-situ process monitoring of the electron-beam melting technology used in additive manufacturing[J]. Proc. SPIE K, 2013, 87050: 87050K-87059K.
[8] Santospirito S P, Słyyk K, Luo B, et al. Detection of defects in laser powder deposition (LPD) components by pulsed laser transient thermography[J]. SPIE Defense, Security, and Sensing, International Society for Optics and Photonics, 2013: 87050X-87050X.
[9] Abd-Elghany K, Bourell D L. Property evaluation of 304L stainless steel fabricated by selective laser melting[J]. Rapid Prototyping Journal, 2012, 18(5): 420-428.
[10] Ding Y, Zhang X, Kovacevic R. A laser-based machine vision measurement system for laser forming[J]. Measurement, 2016, 82: 345-354.
[11] Ding, Y., Huang, W., and Kovacevic, R., An On-line Shape-matching Weld Seam Tracking System, Robotics and Computer-Integrated Manufacturing 42 (2016): 103-112.
[12] Liu R, Liu R, Wang Z, et al. Stereo vision-based repair of metallic components[J]. Rapid Prototyping Journal, 2017, 23(1): 65-73.
[13] Aminzadeh M, Kurfess T. Vision-based inspection system for dimensional accuracy in powder-bed additive manufacturing[C]//ASME 2016 11th International Manufacturing Science and Engineering Conference. American Society of Mechanical Engineers, 2016: V002T04A042-V002T04A042.
[14] Aviles-Viñas J F, Rios-Cabrera R, Lopez-Juarez I. On-line learning of welding bead geometry in industrial robots[J]. The international journal of advanced manufacturing technology, 2016, 83(1-4): 217-231.
[15] Vahabli E, Rahmati S. Application of an RBF neural network for FDM parts' surface roughness prediction for enhancing surface quality[J]. International Journal of Precision Engineering and Manufacturing, 2016, 17(12): 1589-1603.